ISSN 1070-3284, Russian Journal of Coordination Chemistry, 2022, Vol. 48, No. 5, pp. 318–324. © Pleiades Publishing, Ltd., 2022.

Synthesis, Crystals Growth, and Characterization of Methylurea Coordinated Ni(II) and Cu(II) Complexes

T. F. Cao[a, b], X. X. Zhuang[a, *], Z. H. Xu[a], L. W. Ye[a], and D. P. Li[a, b]

[a] *Key Laboratory of Optoelectronic Materials Chemistry and Physics, Fujian Institute of Research on the Structure of Matter, Chinese Academy of Sciences, Fuzhou, 350002 P.R. China*

[b] *College of Chemistry, Fuzhou University, Fuzhou, 350116 P.R. China*

**e-mail: zxx@fjirsm.ac.cn*

Received June 4, 2021; revised October 14, 2021; accepted October 21, 2021

Abstract—New optical coordinated complexes $Cu_xNi_{1-x}(C_2H_6N_2O)_6SO_4$ ($x = 0.31, 0.49, 0.66$) were synthesized and the single crystal $Cu_{0.66}Ni_{0.34}(C_2H_6N_2O)_6SO_4$ (**I**) was selected for characterization. FT-IR and Raman spectroscopic studies were carried out to identify the various functional groups present in crystal. The crystal structure **I** was established by single crystal X-ray diffraction (XRD) technique (CIF file CCDC no. 2068488) and the complex belongs to trigonal system, $R\bar{3}c$ space group. TGA–DTA measurements showed complex **I** remains stable until about 180°C. UV–Vis spectrum of complex **I** exhibited three absorption bands in ultraviolet, visible and near-infrared region, respectively, which was attributed to *d*–*d*, L–M and π–π* transitions absorption. Moreover, the absorption peaks of **I** have a distinct bathochromic shift (20 nm) compared with $M(H_2O)_6^{2+}$ units (M = Ni, Cu). The photophysical properties allow it to selectively filter yellow-green and blue-violet light.

Keywords: methylurea, crystal growth, crystal structure, thermostability, photophysical properties

DOI: 10.1134/S1070328422050025

INTRODUCTION

Transition metal complexes represent an important class of crystalline materials with various properties, for example, used for energy-storage technologies [1, 2], optical devices [3–5] or being a promising dielectric material [6]. In particular, the complexes play a significant role in the application of bandpass filters, an appliance that can accomplish the transmission of specific spectral wavelengths [7, 8]. The potential of hydrated transition metal complexes used as optical bandpass filters were found, originally, such as NSH [9], CUSH [10]. NSH crystals have been applied in UV sensors with satisfactory performance due to its excellent characteristics—high UV spectrum penetration (>85%), narrow band width (200–320 nm) and strong absorption in others [11]. CUSH crystals have a transmission band (280–570 nm), which allows for it to be used as peculiar bandpass filters [12]. These unique filtering properties owe to the electron transitions absorption in $M(H2O)_6^{2+}$ units of the complexes [13, 14]. Studies have shown that similar materials can be derived from these hydrated transition metal complexes with interesting optical properties [15, 16], leading to the attention of researchers having mainly manifested itself in the synthesis of new optical materials that have a wide range of filtration and better thermal stability [17, 18].

In general, there are a variety of ways applied to synthesize these new materials. One of them is to introduce monovalent cations into transition metal salt (such as NH^+, K^+, Na^+), to obtain a Tutton's salt crystal. Potassium cobalt sulfate hexahydrate ($K_2Co(SO_4)_2{\cdot}6H_2O$) crystal was reported [19] with fine UV transmittance (80%) at 200–400 nm. Alternatively, researchers get a mixed optical crystal by doping other transition metal cations. For example, $FeNi(SO_4)_2{\cdot}12H_2O$ [20] and $CoNi(SO_4)_2{\cdot}12H_2O$ [21], which are all in the possession of satisfactory ultraviolet transmittance. In addition, it is an noteworthy approach to replace its water ligands with other molecules that have a stronger coordinating ability with transition metal cation. Se Hun Kim et al. [22] prepared four novel complexes that could be applied in six-primary-color liquid crystal display color filter, in order to improve the color gamut. Cr and Co based metal complexes were synthesized and devoted to violet and red color filters [23]. On the basis of the above research, it can be observed that numbers of new optical materials are synthesized by these ways, which have the prospect of application as bandpass filters.

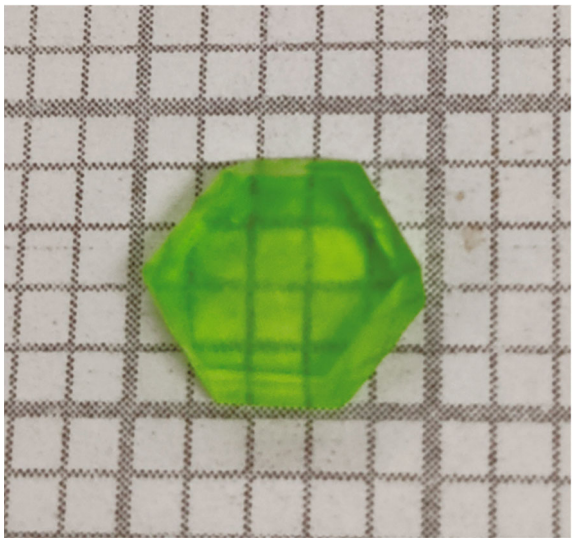

Fig. 1. Photographs of crystal **I**.

In this paper, new optical materials $Cu_xNi_{1-x}(C_2H_6N_2O)_6SO_4$ were synthesized by replacing all six water ligands of hydrated transition metal complexes with methylurea [24], which had high stability and particular UV–Vis spectrum. The bulk single crystals of $Cu_{0.66}Ni_{0.34}(C_2H_6N_2O)_6SO_4$ (**I**) were grown by slow evaporation method. Single crystal XRD and powder XRD were applied to study the structure and purity of **I**, respectively. FT-IR and Raman spectroscopy was used to identify the various functional groups present in the structure **I**. TGA-DTA measurements showed that new complexes remain stable at high temperature. UV–Vis absorption spectrum of **I** were obtained as to study its photophysical properties.

EXPERIMENTAL

Materials and methods. Compounds $NiSO_4·6H_2O$, $CuSO_4·5H_2O$, and methylurea ($C_2H_6N_2O$) were used without further purification. Powder X-ray diffraction (PXRD) was studied by a Miniflex 600 Desktop X-ray Diffractometer with CuK_α (λ = 1.5406 Å) radiation; the sample was scanned in the range of 5°–50° at the rate of 2°/min). The FT-IR spectra and Raman spectroscopic measurements of complex **I** were performed by a Horiba Jobin-Yvon LabRAM Aramis—Raman Spectrometer in the range of 50–2500 cm^{-1}. UV absorption spectra of single crystals (with a thickness of about 3.5 mm) was recorded with a PE-Lambda 950 spectrometer in the wavelength range 200–1200 nm. Thermal gravimetric analysis (TGA) and differential thermal analysis (DTA) measurements of **I** were conducted on a STA449C-QMS403C instrument at a heating rate of 10°C/min from 30 to 800°C under N_2 atmosphere. The grown crystals were subjected to element proportion measurements by an Ultima 2 ICP OES spectrometer and a Vario EL-Cube element analyzer.

Complexes were synthesized in accordance of the following reaction:

$$(1-x)NiSO_4·6H_2O + xCuSO_4·5H_2O + 6C_2H_6N_2O \rightarrow Cu_xNi_{1-x}(C_2H_6N_2O)_6SO_4 + H_2O.$$

Synthesis of complex I. For the preparation of the solution reagents, methylurea were fixed at 44.8 g (0.6 mol), the mass of nickel sulfate and copper sulfate was obtained from the stoichiometric ratio given by the empirical formula $Cu_xNi_{1-x}(C_2H_6N_2O)_6SO_4$. The saturated solution was prepared for 2 h at 60°C. Afterwards the solution was covered with perforate PVC film and then housed in an atmosphere of 60°C to allow solvent evaporation. After 5 days, regular centimeter-sized crystals with optical properties were attained (Fig. 1). The amount of reagents used in crystal growth are presented in Table 1. During the growth of **I** series crystals, a small amount of by-product $(NH_4)_2Ni(SO_4)_2·6H_2O$ can be observed, and which is difficult to be avoided by evaporation method. Thus, the increase of nickel sources can promote the growth of $(NH_4)_2Ni(SO_4)_2·6H_2O$, leading to product crystals of more macroscopic defects. This makes the decrease of distribution coefficient (Ni). As a result, complex **I** was selected for subsequent characterization testing.

IR data for **I** (KBr; ν, cm^{-1}): 3422, 3317, 2945, 2839, 1645, 1595, 1573, 1416, 1373, 1173, 1117, 773, 619, 528.

The X-ray structure determination. X-ray crystallographic data were collected on a Rigaku UltraX-Sat-

Table 1. The preparation data of growth solution and the element proportion for **I**, **Ia**, **Ib**

Group	**I**	**Ia**	**Ib**
$NiSO_4·6H_2O$ (mol)	0.03	0.05	0.07
$CuSO_4·5H_2O$ (mol)	0.07	0.05	0.03
The proportions of Ni^{2+}/Cu^{2+}	0.34 : 0.66	0.51 : 0.49	0.69 : 0.31
Anal. calcd., % (C, H, N)	23.9, 6.0, 27. 9	24.0, 6.0, 27.9	24.0, 6.0, 28.0
Found, % (C, H, N)	23.8, 5.9, 27.6	23.9, 6.0, 27.8	23.9, 6.0, 27.9
Main product	$Cu_{0.66}Ni_{0.34}(C_2H_6N_2O)_6SO_4$	$Cu_{0.49}Ni_{0.51}(C_2H_6N_2O)_6SO_4$	$Cu_{0.31}Ni_{0.69}(C_2H_6N_2O)_6SO_4$

Table 2. Crystallographic data and structure refinement details for **I**

Parameter	Value
Chemical formula	$C_{12}H_{36}N_{12}O_6Cu_{0.66}Ni_{0.34}{\cdot}SO_4$
M_r	602.68
Crystal system; space group	Trigonal; $R\bar{3}c$
Temperature, K	293
a, Å	10.9701(5)
c, Å	40.377(4)
V, Å^3	4208.1(5)
Z	6
S	1.167
F(000)	1902
Range for data collections θ, deg	2.2023–27.5010
Limiting indices	$-14 \le h \le 14$, $-14 \le k \le 14$, $-52 \le l \le 52$
μ, mm^{-1}	0.917
Crystal size, mm	0.4 × 0.5 × 0.6
T_{min}, T_{max}	0.9186, 1.0000
Reflections collected/unique	10205/1077
R_{int}	0.0292
Reflections with $I > 2\sigma(I)$	1027
Data/restraints/parameters	1077/57/94
Goodness-of-fit on F^2	1.167
R indices (all data)	$R_1 = 0.0334$, $wR_2 = 0.0896$
Final indices ($I > 2\sigma(I)$)	$R_1 = 0.0309$, $wR_2 = 0.0874$
$\rho\Delta_{max}/\rho\Delta_{min}$, e/A^3	0.211/–0.270

urn724 small molecule single crystal X-ray diffractometer with MoK_α (λ = 0.71073 Å) radiation. The structure was resolved by direct methods with the computer program SHELXT-2018/2 and refined by a full-matrix least-squares refinement on F^2 with the computer program SHELXL-2018/3 as programmed in the software suite Olex 2 [25, 26]. Crystal data and structure refinement details for **I** are summarized in Table 2. The bond lengths and bond angles data are listed in Table 3.

Supplementary material for structure **I** has been deposited with the Cambridge Crystallographic Data Centre (no. 2068488; deposit@ccdc.cam.ac.uk or http://www.ccdc.cam.ac.uk).

RESULTS AND DISCUSSION

In structure **I**, M (Ni^{2+}/Cu^{2+}) serves as the coordinate center in one repeating unit (Fig. 2). The coordinate center is surrounded by six oxygen, which from the carbonyl group of methylurea. $M(C_2H_6N_2O)_6^{2+}$ unit (M = Ni, Cu) proved to be an approximately regular octahedron, in accordance with the bond lengths and bond angles data (Table 3). Two kinds of hydrogen bonds are in this structure (Fig. 2b), one is between methylurea ligands and the sulfate anions, the other is between the H in the amino group and the O in the

Table 3. Selected geometric parameters (Å, deg) for **I***

Bond	*d*, Å	Bond	*d*, Å
M–O(1)	2.0747(12)	M–O(1e)	2.0748(12)
M–O(1a)	2.0748(12)	O(1)–C(1)	1.261(2)
M–O(1b)	2.0748(12)	N(1)–C(1)	1.327(2)
M–O(1c)	2.0748(12)	N(2)–C(1)	1.327(2)
M–O(1d)	2.0748(12)	N(2)–C(2)	1.443(3)
Angle	ω, deg	Angle	ω, deg
O(1)MO(1c)	180.00(7)	O(1a)MO(1d)	180.000
O(1b)MO(1e)	180.000		

* Symmetry codes: (a) $x - y + 1/3$, $x - 1/3$, $-z + 2/3$; (b) $y + 1/3$, $-x + y + 2/3$, $-z + 2/3$; (c) $-x + 4/3$, $-y + 2/3$, $-z + 2/3$; (d) $-x + y + 1$, $-x + 1$, z; (e) $-y + 1$, $x - y$, z.

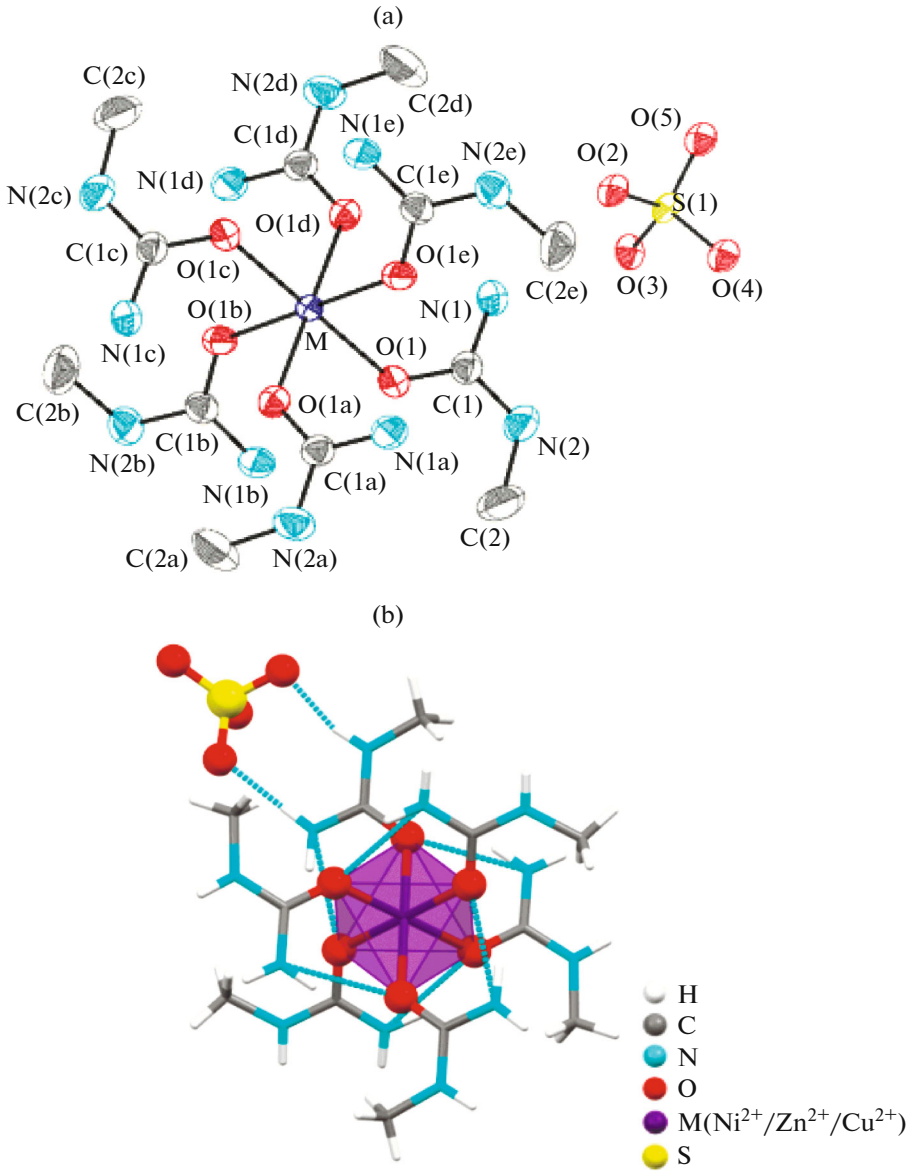

Fig. 2. The coordination environment of the M (Ni^{2+}/Cu^{2+}) in **I**, shown with 30% probability displacement ellipsoids. H atoms have been omitted for clarity (a); illustration of the hydrogen bonds in structure **I** (b).

carbonyl group of different methylurea ligands. Both hydrogen bonds can improve the thermal stability of the compounds.

Complex **I** was subjected to PXRD analysis. As shown in the Fig. 3, the test results demonstrate that the peaks measured by PXRD are fully overlapped with the ones calculated by Mercury, which indicates the as-synthesized sample with a high purity. In addition, well sharp and strong peaks observed in Fig. 3, illustrating the fact that the grown crystals are of high crystallinity [27].

The FT-IR spectra of complex **I** are shown in Fig. 4a. Among the bands, two peaks at 1117 and 619 cm^{-1} are the absorption of S–O stretching vibrations in the sulfate anions [28]. The pointed peaks at 3422 and 3317 cm^{-1} are due to stretching vibrations of N–H and the band at 1645 is assigned to C=O stretching vibration in the amide [18]. All these bands demonstrate the presence of methylurea and sulfate anions in the structure of **I**.

In order to prove the existence of octahedral complexes $M(C_2H_6N_2O)_6$, the Raman spectroscopic measurements of **I** and methylurea were performed in the range of 50–2500 cm^{-1}. The sharp peaks can be observed (Fig. 4b), which further indicates the crystallinity of **I** is high. Compared with methylurea, there are a few extra characteristic peaks in **I** at 224, 390, 536, 676, 984, 1130 cm^{-1}. Among the rest, the peaks

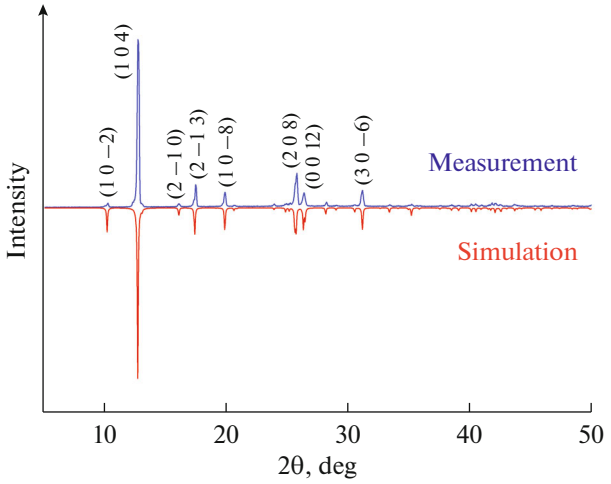

Fig. 3. Powder X-ray diffraction patterns for complex **I** (blue: measurement, red: simulation).

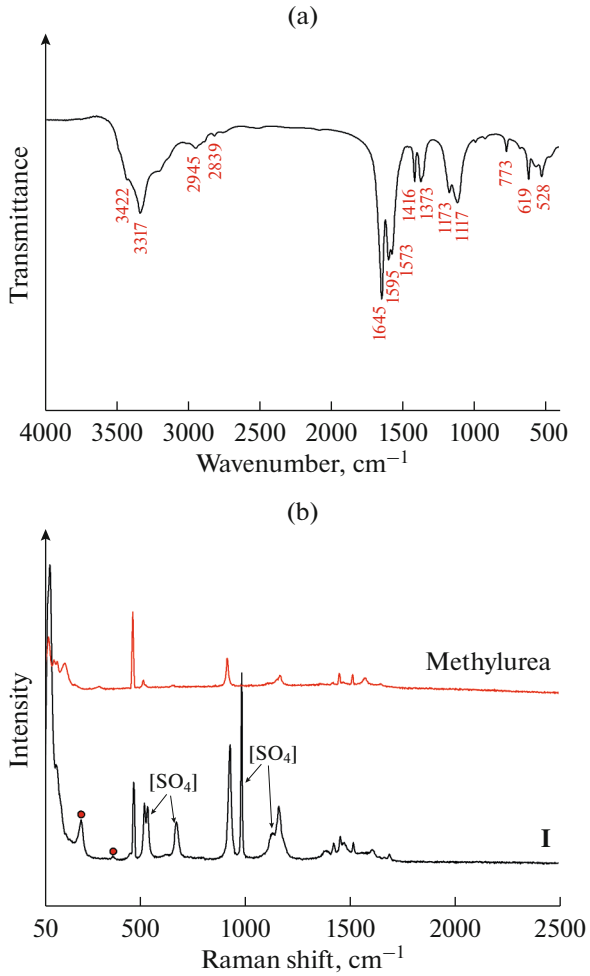

Fig. 4. FT-IR spectrum of complex **I** (a); Raman spectrum of complex **I** and methylurea (b).

are due to the vibration of sulfate anions at 536, 676, 984, 1130 cm^{-1} [26]. The vibration of the octahedral complexes $M(H_2O)_6^{2+}$ are at 393.8, 256.5, 238.2, 228 cm^{-1}. Therefore, we make a judgment that the peaks at 224, 390 cm^{-1} may attribute to the vibration of $M(C_2H_6N_2O)_6$ (M = Ni, Cu) [29, 30].

The results of the TGA-DTA measurements are plotted in Fig. 5. Crystal starts to decompose at 180°C around, which means a terrific thermostability. The TG analysis of complex **I** shows three steps of mass loss in a total of 87.12% (theor. loss, 86.73%). The first two mass loss of total 74.33% occurred between 180–300°C correspond to the decomposition of methylurea molecule (theor. loss, 73.75%). The mass loss of 12.79% in the range of 300–600°C attributed to the decomposition of sulfate anions, it can be due to the release of one sulfur trioxide molecule (theor. loss, 12.97%) [16, 31, 32].

The data for the UV absorption peaks of samples were listed in Table 4. As depicted in Fig. 6, three absorption bands in sight, due to the *d*–*d*, L–M and π–π* transitions in $M(C_2H_6N_2O)_6^{2+}$ (M = Ni, Cu) [33]. The absorption band from 400 to 420 nm is derived from methylurea to metal charge transfer bands in the octahedral field of $Cu(C_2H_6N_2O)_6^{2+}$ and the bands of $^3A_{2g}(^3F) \rightarrow {}^3T_{1g}(^3F)$ transitions in $Ni(C_2H_6N_2O)_6^{2+}$ unit [34]. The near-infrared absorption band from 750 to 1000 nm is interpreted as the vertical transitions, $^3A_{2g}(^3F) \rightarrow {}^3T_{1g}(^3P)$ of Ni^{2+} ion and $^2E_g \rightarrow {}^2T_{2g}$ of Cu^{2+} ion [35]. In besides, the absorption band from 200 to 360 nm may be associated with π→π* transitions in metal-ligand bonding of $M(C_2H_6N_2O)_6^{2+}$ (M = Ni, Cu) [36]. Compared with $M(H_2O)_6^{2+}$ (M = Ni, Cu) [9, 10], the bathochromic shifts should be caused by the coordination ability of methylurea, which leads to a lower energy requirement for the electron transitions, in $M(C_2H_6N_2O)_6^{2+}$ units

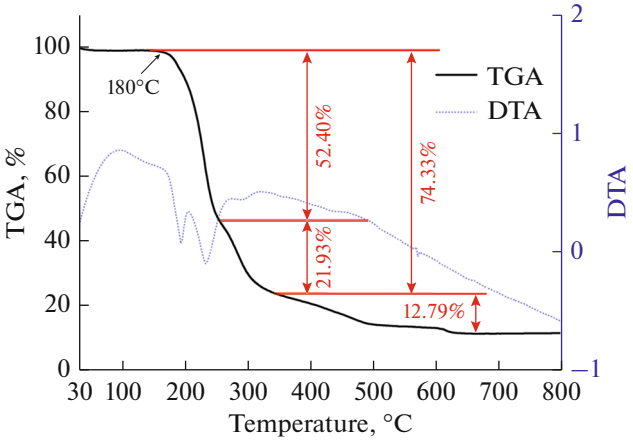

Fig. 5. TGA and DTA curve for complex **I**.

Table 4. Wavelength at absorption peaks for samples

Sample	Absorption band, nm	Electronic transitions
I	400–420	$[Ni(C_2H_6N_2O)_6]^{2+}$: $^3A_{2g}$ (^3F) → $^3T_{1g}$ (^3P)
		$[Cu(C_2H_6N_2O)_6]^{2+}$: Ligand to metal charge transfer
	750–1000	$[Ni(C_2H_6N_2O)_6]^{2+}$: $^3A_{2g}$ (^3F) → $^3T_{1g}$ (^3F)
		$[Cu(C_2H_6N_2O)_6]^{2+}$: ^2E_g → $^2T_{2g}$
NSH	380–450	$[Ni(H_2O)_6]^{2+}$: $^3A_{2g}$ (^3F) → $^3T_{1g}$ (^3P)
	670–820	$[Ni(H_2O)_6]^{2+}$: $^3A_{2g}$ (^3F) → $^3T_{1g}$ (^3F)
CUSH	600–1150	$[Cu(H_2O)_6]^{2+}$: ^2E_g → $^2T_{2g}$

(M = Ni, Cu) [37]. These photophysical properties allow it to selectively filter yellow-green and blue-violet light.

Thus, new complexes $Cu_xNi_{1-x}(C_2H_6N_2O)_6SO_4$ (x = 0.31, 0.49, 0.66) were synthesized. Bulk single crystal **I** with the best crystal quality was selected for characterization. The existence of sharp-narrow peaks in X-ray diffractogram and Raman spectrum confirmed the crystallinity of complexes. Two kinds of hydrogen bonds in this structure are different from hydrated transition metal complexes, which makes the structure of compounds more stable. The high heat resistance (180°C) of **I** was verified. UV–Vis spectra showed three absorption bands in ultraviolet (200–360 nm), visible (411 nm) and near-infrared (800–1000 nm) region for **I**, respectively. Compared with $Ni(H_2O)_6^{2+}$ and $Cu(H_2O)_6^{2+}$, the bathochromic shifts (20 nm) of characteristic peaks were due to the coordination ability of methylurea, which leads to a lower energy requirement for the electron transitions in $M(C_2H_6N_2O)_6^{2+}$ unit (M = Ni, Cu). The present investigation clearly shows that the titled methylurea coordinated Ni(II) and Cu(II) single crystal is an optical material which can selectively filter the light at a particular wavelength with the good stability.

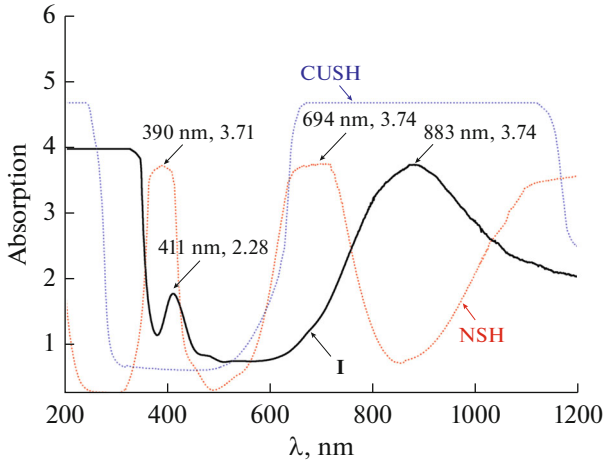

Fig. 6. UV absorption spectrum of **I**, NSH, and CUSH.

FUNDING

This research did not receive any specific grant from funding agencies in the public, commercial, or not-for-profit sectors.

CONFLICT OF INTEREST

The authors declare that they have no conflicts of interest.

REFERENCES

1. Canto-Aguilar, E.J., Oliver-Tolentino, M.A., Guadalupe Ramos-Sanchez, et al., *Electrochim. Acta*, 2021, vol. 371, p. 137828.
2. Qi Zheng, Zhihui Niu, Jing Ye, et al., *Adv. Func. Mater.*, 2017, vol. 27, no. 4, p. 1.
3. Singh, D., Nehra, K., Saini, R.K., et al., *Optik*, 2020, vol. 206, p. 164338.
4. Ahmad, M., Manzoor, K., Ahmed, S., et al., *Optik*, 2016, vol. 127, no. 10, p. 4329.
5. Füreya Elif Özbek, Mustafa Yüksek, and Hacali Necefoğlu, *Optik*, 2016, vol. 127, no. 19, p. 7710.
6. Ramteke, S.P., Anis, M., Baig, M.I., et al., *Optik*, 2018, vol. 154, p. 275.
7. Xinxin Zhuang, Genbo Su, Guofu Wang, et al., *Cryst. Res. Technol.,* 2004, vol. 39, no. 9, p. 754.
8. Ghosh, S., Oliveira, M., Pacheco, T.S., et al., *J. Cryst. Growth*, 2018, vol. 487, p. 104.
9. Mathpal, S. and Kandpal, N.D., *E.-J. Chem.*, 2009, vol. 6, p. 445.
10. Manomenova, V.L., Stepnova, M.N., Grebenev, V.V., et al., *Crystallogr. Rep.*, 2013, vol. 58, p. 513.
11. Wang Wen-Ting, Xu Zhi-Huang, Ye Li-Wang, et al., *Chinese J. Struct. Chem.*, 2017, vol. 36, p. 12.
12. Anandalakshmi, H., Parthiban, S., Parvathi, V., et al., *J. Therm. Anal. Calorim.*, 2011, vol. 104, p. 963.
13. Prostomolotov, A.I., Verezub, N.A., Vasilyeva, N.A., and Voloshin, A.E., *Crystals*, 2020, vol. 10, p. 982.

14. Rudneva, E.B., Manomenova, V.L., Malakhova, L.F., et al., *Crystallogr. Rep.*, 2006, vol. 51, p. 344.
15. Chena, J.W., Wang, X.Q., and Ren, Q., *Optik*, 2015, vol. 126, p. 3025.
16. El-Fadla, A., Maini, L., Tatarchuk, T., et al., *Vibration. Spectrosc.*, 2019, vol. 104, p. 102942.
17. Pacheco, T.S., Ludwig, Z.M.C., Sant' Anna, D.R., et al., *Vibration. Spectrosc.*, 2020, vol. 109, p. 103093.
18. Wenting Wang, Zhihuang Xu, Liwang Ye, et al., *Crystals*, 2017, vol. 7, p. 68.
19. Dyatlova, N.A., Manomenova, V.L., Rudneva, E.B., et al., *Crystallogr. Rep.*, 2013, vol. 58, p. 749.
20. Genbo Su, Xinxin Zhuang, Youping Hea, et al., *J. Cryst. Growth*, 2002, vol. 243, p. 238.
21. Genbo Su, Xinxin Zhuang, Youping He, et al., *Cryst. Res. Technol.*, 2003, vol. 38, p. 1087.
22. Kim, S.H., Namgoong, J.W., Yuk, S.B., et al., *J. Incl. Phenom. Macrocycl. Chem.*, 2015, vol. 82, p. 195.
23. Seok, C.H., Jaung, J.Y., Park, J., et al., *Mol. Cryst. Liquid Cryst.*, 2010, vol. 529, p. 80.
24. Nardelli, M., and Coghi, L, *Gazz. Chim. Ital.*, 1958, vol. 88, p. 355.
25. Dolomanov, O.V., Bourhis, L.J., Gildea, R.J., et al., *J. Appl. Crystallogr.*, 2009, vol. 42, p. 339.
26. Sheldrick, G.M., *Acta Crystallogr., Sect. C: Struct. Chem.*, 2015, vol. 71, p. 3.
27. Anbuchezhiyan, M., Ponnusamy, S., Singh, S.P., et al., *Cryst. Res. Technol.*, 2010, vol. 45, p. 497.
28. Bejaoui, A., Souamti, A., Kahlaoui, M., et al., *Mater. Sci. Eng., B*, 2019, vol. 240, p. 97.
29. Pacheco, T.S., Ludwig, Z.M.C., Ghosh, S., et al., *Mater. Res. Express*, 2019, vol. 6, p. 096302.
30. Ghosh, S., Ullah, S., de Mendonca, J.P.A., et al., *Spectrochim. Acta, A*, 2019, vol. 218, p. 281.
31. Tomaszewicz, E. and Kotfica, M., *J. Therm. Anal. Calorim.*, 2004, vol. 77, p. 25.
32. Gadalla, A.M., *J. Chem. Kinetics*, 1984, vol. 16, p. 655.
33. Komaei, S.A., van Albada, G.A., and Reedijk, J., *Transition Met. Chem.*, 1999, vol. 24, p. 104.
34. Jagvir Singh, Anu, and NetraPal Singh, *J. Spectrosc.*, 2013, vol. 213, p. 792318. https://doi.org/10.1155/2013/792318
35. Dick, A., Rahemi, H., Krausz, E.R., et al., *J. Chem. Phys.*, 2008, vol. 129, p. 214505.
36. Ghosh, S., Lima, A.H., Flôres, L.S., et al., *Opt. Mater.*, 2018, vol. 85, p. 425.
37. Gao Sheng-Min, Xu Zhi-Huang, Ye Li-Wang, et al., *Chinese J. Struct. Chem.*, 2015, vol. 34, p. 1682.